Search for a ferroelectrically ordered form of ice VII by neutron diffraction under high pressure and high electric field

R. Yamane,[1,*] K. Komatsu,[1] H. E. Maynard-Casely,[2] S. Lee,[2] N. Booth,[2] and H. Kagi[1]

[1]*Geochemical Research Center, Graduate School of Science, The University of Tokyo, Hongo 7-3-1, Bunkyo-ku, Tokyo 113-0033, Japan*

[2]*Australian Nuclear Science and Technology Organisation (ANSTO), Locked Bag 2001, Kirrawee DC, 2234 New South Wales, Australia*

(Received 30 July 2018; revised manuscript received 17 March 2019; published 3 May 2019)

Neutron diffraction experiments of ice VII at pressures up to 6.2 GPa and 10.2 kV/mm were conducted to investigate the potential ferroelectrically ordered structure of ice VII induced by a high electric field. To accomplish this, we developed a high-pressure cell assembly to allow for powder neutron diffraction to be conducted under both high-pressure and high-electric field conditions. However, the subsequent observed diffraction patterns taken *in situ* at these conditions do not show sufficient evidence of the proposed ferroelectrically ordered structure of ice VII. We estimate the degree of the hydrogen ordering in ice VII under the applied conditions from high-pressure *P-E* loop measurements, and discuss the future possibilities of detecting the ferroelectrically ordered structure.

DOI: 10.1103/PhysRevB.99.174201

A single water molecule has an electric dipole moment; the dielectric properties derived from this dipole moment are a relatively unexplored parameter in the investigations of water ice's many polymorphs (e.g., [1–3])—18 phases are known to date [4]. The 18 polymorphs are classified into hydrogen disordered and ordered phases, and this classification directly relates to the degree of ordering of dipole moments. The majority of ordered ice polymorphs have a nonpolarized structure, in other words, their structures possess a center of symmetry. The exceptions to this are ice XI (the ordered form of ice Ih) [5] and ice XV (the ordered form of ice VI though its structure is still under debate [3,6–8]).

The structure of ice VII includes disordered hydrogen atoms within the structure (space group $Pn\bar{3}m$) shown in Fig. 1 and has long been considered as a single phase in the wide stability region, from 2 to 60 GPa at room temperature. However, several anomalous phenomena are observed between 10 and 15 GPa by a number of different methods, and these anomalies have caused questions for the single-phase scenario of ice VII. For example, Pruzan *et al.* reported that a width of a Raman-scattering peak, corresponding to a symmetric vibration mode of a water molecule, has a minimum at around 10 GPa [9]. Somayazulu *et al.* showed a peak splitting in an x-ray-diffraction pattern at 14.8 GPa [10]. Fukui *et al.* reported that x-ray-induced dissociation yield of ice VII has a maximum at 14 GPa from x-ray Raman spectra [11]. The anomalies even extend into the physical properties: Okada *et al.* show that a pressure dependence of electric conductivity of ice VII has a maximum at 12 GPa from the impedance measurements [12]. More recently, Noguchi *et al.* showed a maximum in self-diffusion coefficients using micro-Raman spectroscopy at around 11 GPa [13]. Although previous studies suggested a possibility that a pressure-induced partial ordering occurs at around 10–15 GPa [9,10], no comprehensive interpretation for the experimental anomalies has been found.

The ordered form of ice VII is ice VIII, which has an antiferroelectrically ordered structure (called "AFE structure" hereafter, and its crystal structure is shown in Fig. 1, space group $I4_1/amd$). The AFE structure has been considered as a candidate for the partially ordered structure in ice VII (if ice VII is really partially ordered). However, Caracas and Hemley [15] have proposed a different scheme for the partial ordering of ice VII by using density functional theory calculations. They proposed that a ferroelectrically ordered structure (called "FE structure" hereafter, and its crystal structure is shown in Fig. 1, space group $P4_2nm$) could occur in ice VII at a bulk scale under high-electric field. Their calculations show that the AFE structure is slightly more stable than the FE structure, but the energy difference between AFE and FE structures was so small (∼10 meV/molecule [15]) that the FE structure could be stabilized under an external electric field. Their calculation also shows that the energy difference slightly decreases from 12.3 meV/molecule at 2 GPa to 11.7 meV/molecule at 10 GPa with increasing pressure. The energy difference between FE and AFE is almost comparable below 10 GPa; it will be predicted, from the estimated volume fraction of the FE structure at pressure lower than 10 GPa, how much the ferroelectrical ordering is induced by high electric field in ice VII above 10 GPa. In this study, high-pressure and high electric-field neutron experiments were conducted at up to 6.2 GPa with overcoming some technical difficulties as mentioned later. If the FE structure is found experimentally, the discovery will contribute not only for the understanding of the anomalies observed in ice VII but also in the knowledge of how orientations of water molecules affect ice structure, stability, and other physical properties.

Neutron diffraction experiments under high pressure and high electric field would be the most direct method to find

*yamane@eqchem.s.u-tokyo.ac.jp

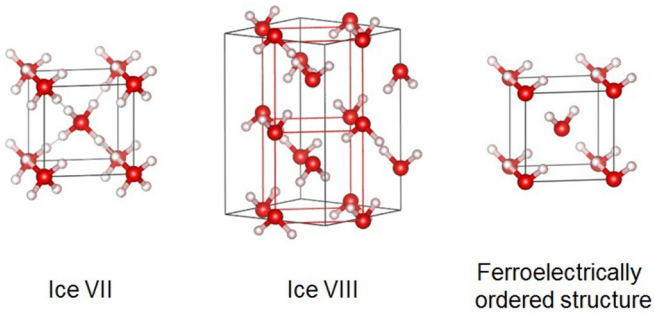

FIG. 1. Crystal structures, ice VII, ice VIII, and hypothetical ferroelectrically ordered structure (FE structure). The black lines show the unit cells and the red line in ice VIII corresponds to the unit cell of ice VII. (The crystal structures were drawn by VESTA developed by Momma and Izumi [14]).

the FE structure, however such measurements had previously been technically unfeasible. In general, cooperative phenomena among dipoles are induced by electric field in an order of kV/mm across samples of order tens to hundreds μm thickness as this enables a large electrical field to be generated with a limited voltage. This is rather incompatible with the thin samples required to achieve high pressures. Additionally, neutron diffraction requires larger volume samples, at least a few mm^3, to obtain sufficient diffraction intensity, because of the relatively weak nature of neutron sources. A further difficulty is that the electrodes to apply a high electric field have to be electrically insulated, challenging in the close confines of a high-pressure cell.

We recently overcame these technical difficulties and developed a cell assembly for *in situ* neutron diffraction experiments under high-pressure and high electric fields, and here we present neutron diffraction patterns of ice VII at room temperature, at pressures up to 6.2 GPa and at electric field up to 10.2 kV/mm.

A picture and schematic drawings of the developed cell assembly are shown in Fig. 2(a). Double-toroidal type anvils were used to generate high pressure. The anvils are made of sintered diamond [abbreviated "SD" in Fig. 2(a)] with a cobalt binder, which works as an electric conductor. A coupled pair of spherical caps of TiZr null scattering alloy attached to the anvils with silver paste were used as electrodes in order to reduce scattering from the anvils and also to make electrodes parallel. The upper side of the anvil was electrically insulated from a high-pressure press by using a PTFE collar and mica sheets (see more details in [16]). Heat-treated pyrophyllite rings (700 °C, 1 h) were used as gaskets, as it was found that non-heat-treated pyrophyllite gaskets caused electrical breakdown at around 1.5 kV/mm, probably due to the hydrous component [Fig. 2(b)] [17]. The inner PTFE ring was used to seal the water sample under initial loading and the outer PTFE ring works to ensure uniform deformation of the heat-treated pyrophyllite gasket under compression.

Neutron diffraction experiments were carried out on the High Intensity Powder Diffraction instrument, WOMBAT, at the ANSTO. The wavelength of neutrons used was 1.885 Å. A small radial collimator [Fig. 2(c)], having partitions made of Gd_2O_3 painted thin film, was set on the Paris-Edinburgh press to reduce the parasitic scattering from the high-pressure

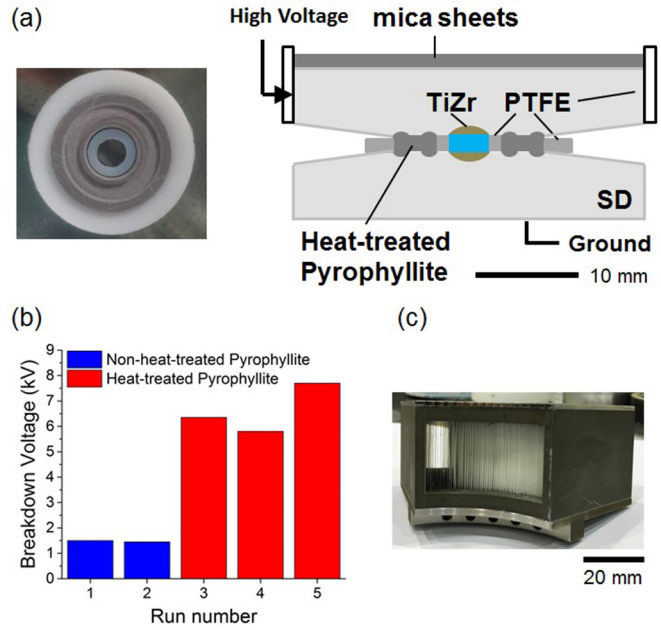

FIG. 2. (a) Schematic drawings of cross section for a developed double-toroidal-type anvil cell assembly (right) and the picture of gaskets (left), where SD and PTFE denote sintered diamond and polytetrafluoroethylene, respectively. Samples, with a volume ~20 mm^3, are loaded into the gaskets sandwiched by anvils, and compressed using a Paris-Edinburgh press (type VX5). The upper anvil was electrically connected to a high-voltage power supply, and was insulated from the press by using the PTFE collar and mica sheets. The bottom anvil was electrically grounded. (b) Breakdown voltages of the five experimental runs, by using non-heat-treated pyrophyllite (blue) and heat-treated pyrophyllite (red). (c) A picture of radial collimator developed for the Paris-Edinburgh press. Each partition of the radial collimator is made of Gd_2O_3-painted thin film. This was used to reduce the measured scattering contribution from the cell assembly.

cell. Deuterated water (99.9%, Wako) was used as a sample and compressed at room temperature. Pressure was estimated from the observed unit-cell volume of ice VII using the third-order Birch equation [18]. High voltage was applied to the electrically insulated upper side of the anvil using a high-voltage power supply (Matsusada AU-10R120). An electrode separation was measured in a separate run using a laser displacement sensor (KEYENCE, IG-028) (black square in Fig. 3). The reproducibility of sample pressure to the applied load in both the neutron and the additional experiments was confirmed by water → ice VI phase transition observed by *in situ* dc resistivity measurements of the samples (red triangle in Fig. 3).

Experimental conditions, pressure, applied voltage, and electrode separation are listed in Table I.

Neutron diffraction patterns at 6.2 GPa, the highest pressure we obtained, with applying electric fields up to 10.2 kV/mm are shown in Fig. 4. All visible peaks in the diffraction patterns can be indexed as 110, 111, and 211 reflections of ice VII, or 110 of diamond (anvils). The FE structure would give two peaks at around 70° and 80° 2θ as discussed later. As it can be seen, these additional peaks were

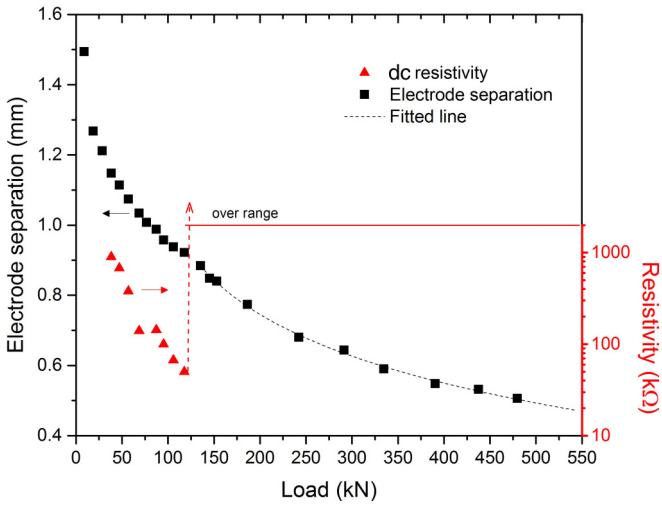

FIG. 3. Electrode separation (black square) and dc resistivity (red triangle) at respective loads. The electrode separation was estimated from anvil gap and the dc resistivity between two anvils was measured using an Iso-Tech IDM73 multimeter. The water → ice VI phase transition was observed in both measurements at around 130 kN. The dotted line is a polynomial fit to electrode-separation data above 130 kN.

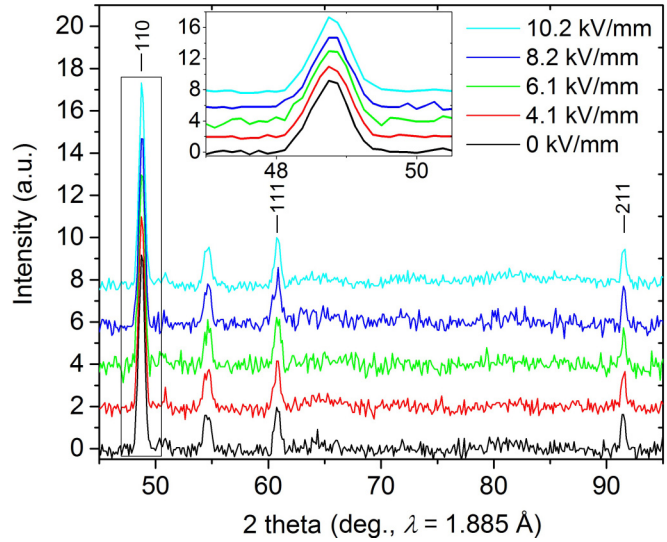

FIG. 4. Neutron diffraction patterns at 6.2 GPa and with 0, 4.1, 6.1, 8.2, and 10.2 kV/mm. Exposure times were 1, 1, 0.5, 0.5, and 2 h, respectively. These conditions of electric field are estimated from the applied voltage and the electrode separation at respective pressures from the line drawn in Fig. 3. The inset shows expanded plots at around 50°. From lower angle, 110, 111, and 211 reflections of ice VII are observed. The peak at around 55° is 110 reflection of diamond (anvils). The undulation from 60° to 90° could be derived from inhomogeneous gaps of the radial-collimator partitions.

not observed in the diffraction patterns at any pressure and electric-field conditions.

We note that the noise level of the observed diffraction patterns are comparable to the Bragg peaks, although the developed radial collimator significantly reduced the parasitic scattering from the cell. It is still possible that the peaks derived from the FE structure may be hidden under the noise level. Consequently, to discriminate this, we simulated how the FE structure could be observed in neutron diffraction patterns. If the FE structure is locally formed in ice VII, the ordered region would increase with increasing electric field. This partially ordered state could be described by a mixed phase model of completely disordered ice VII and completely ordered FE structure. In this model, the FE structure coexists as a domain structure with ice VII.

The mixed phase model of ice VII and the FE structure was simulated at a number of volume fractions (f) of the FE phase using GSAS [19] with EXPGUI [20] (Fig. 5). From this, we could estimate that, considering the noise level of the diffraction pattern, the volume fraction of the FE structure should be less than 0.10 if it was present in the 6.2-GPa and 10.2-kV/mm sample. The intensity of the 210 reflection in the case of $f = 0.10$ should be 1.5 times higher than the averaged noise level, hence this reflection should be visible if f is larger than 0.10.

The volume fraction of the FE structure can also be estimated from electric-field-induced polarization. When an electric field is applied to ice VII, electric polarization, related to the volume fraction, increases corresponding to the dielectric

TABLE I. Pressure, applied voltage, and electrode separation conditions.

Pressure (GPa)	Voltage (kV)	Electrode separation (mm)
3.2	1.5, 2.0, 2.5, 3.0, 3.5, 4.0, 4.5, 5.0	0.68
4.9	2.0, 3.0, 4.0, 5.0	0.57
6.2	2.0, 3.0, 4.0, 5.0	0.49

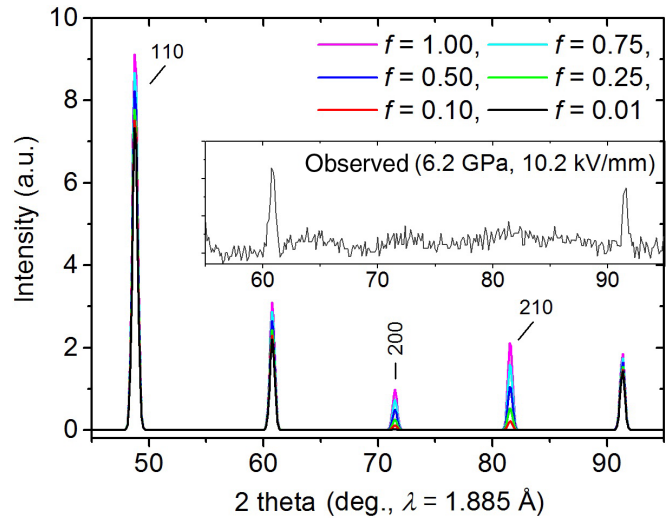

FIG. 5. Simulated neutron diffraction patterns of the mixed phase of ice VII and completely ordered FE structure (space group: $Pn\bar{3}m$ and $P4_2nm$). f represents a volume fraction of FE structure. Inset shows the observed diffraction pattern at 6.2 GPa and 10.2 kV/mm at around 60°–90°. 200 and 210 peaks appear with increasing the volume fraction of FE structure.

constant of ice VII and the strength of the electric field. This polarization causes experimentally observable induced charge on electrodes attached to ice VII. Hereafter we introduce approximate relationship between the volume fraction and electric polarization in ice VII and estimate the volume fraction in light of measurements of electric polarization, which is more sensitive to increases of the volume fraction.

Electric polarization (**P**) is found by a summation of dipole moments in a unit volume: $\mathbf{P} = \sum_i \boldsymbol{\mu}_i$, where i is an index of a water molecule, and $\boldsymbol{\mu}_i$ means a dipole moment of ith water molecule. In the case of ice VII, which possesses center symmetry, the summation of $\boldsymbol{\mu}_i$ is canceled out by disordered orientation of water molecules under zero electric field. If the orientation of the electric field is defined as the z axis, $P = |\mathbf{P}| = \sum_i (\mu_z)_i$ holds, where $(\mu_z)_i$ means a z component of $\boldsymbol{\mu}_i$. Hereafter $|\boldsymbol{\mu}_i|$ is considered as μ ($=6 \times 10^{-22}$ μC cm), the strength of a dipole moment of a water molecule in a gas phase at room temperature and ambient pressure, for any ith water molecule. In order to derive the volume fraction of the FE structure from the polarization, we assumed that the polarization P is all contributed from completely oriented water molecules of the FE structure along electric field,

$$P = \mu N_p, \tag{1}$$

where N_p is a hypothetical number density of the completely oriented water molecules. Additionally, let N ($=6 \times 10^{22}$ cm^3) be a number density of water molecules in ice VII, which can be calculated using the equation of state of ice VII [18], and then N_p/N can be considered to be equal to the volume fraction. We obtain a relationship between the volume fraction and electric polarization;

$$f = P/\mu N. \tag{2}$$

Electric polarization was measured at high pressure by using a differentcell assembly, improved from our previous development using hole-type opposed anvils (see [21] and the Supplemental Material [22]). A notable feature of this cell is that only the sample is sandwiched by electrodes, and this feature allow us to measure induced charge on the electrodes derived from the sample. Electric polarization was observed by *P-E* loop methods using an op-amp-type Sawyer-Tower circuit with 50-Hz ac high voltage. The results of the *P-E* loop measurements at 6.1 GPa with ac electric fields, 2, 4, 6, 8, and 10 kV/mm, are shown in Fig. 6(a). Ice VIII data at 263 K with 10 kV/mm is also shown for comparison to electric polarization of ice VII. Typical paraelectric behavior was observed in ice VII; the observed electric polarization was induced by electric field linearly, though our data show as ellipsoid due to a contribution from the electric conductive component of ice VII. In ice VIII, on the other hand, electric polarization was not induced. This is consistent with the antiferroelectric-type crystal structure of ice VIII and a previous dielectric study of ice VIII reported by Whalley *et al.* [2]. Electric polarization of 2, 4, 6, 8, and 10 kV/mm at each ac electric field is shown in Fig. 6(b). The right axis shows the volume fraction calculated using Eq. (2) and the volume fraction is estimated as about $f = 0.02$ at 6.1 GPa with 10 kV/mm [23]. In this order of the volume fraction, the expected reflections from the FE structure would be hidden in our neutron diffraction experiments. It should be noted that the

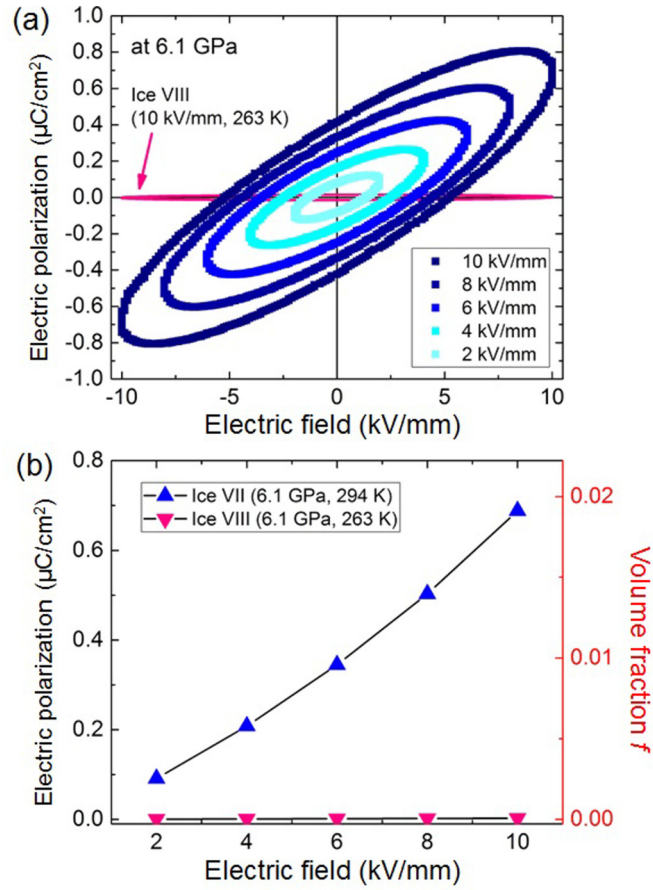

FIG. 6. (a) *P-E* loops at 6.1 GPa with 2, 4, 6, 8, and 10 kV/mm ac electric field. The pink loop corresponds to ice VIII at 263 K with 10 kV/mm. Temperature was measured by *K*-type thermocouple attached to the surface of opposed anvils. (b) Electric-field dependence of electric polarization and the calculated volume fraction using Eq. (2). Electric polarization under 2, 4, 6, 8, and 10 kV/mm is shown at each applied ac electric fields.

polarization of the FE structure is not only oriented along the z axis, but also has different orientations, as the sample was polycrystalline. This means that actual contribution of the FE structures with different orientations to the polarization would be lower than the case of Eq. (1). In other words, a more locally formed FE structure should contribute to yield the polarization P and the calculated volume fraction by Eq. (2) would be underestimated.

When higher electric fields are applied, for example 30 and 50 kV/mm, the f would increase 0.06 and 0.11 from linear extrapolation of the electric-field dependence of the volume fraction shown in Fig. 6(b). At 50 kV/mm, a peak height ratio (the strongest 110 reflection):(the 210 reflection), is 30:1, so that the 210 peak would be observable considering the signal/noise ratio.

In conclusion, we have carried out neutron diffraction experiments of ice VII under both the developed high-pressure and high electric fields of up to 10.2 kV/mm. This was achieved by using a developed high-pressure cell assembly. No clear evidence of the appearance of the ferroelectrically ordered structure was obtained from the observed diffraction

patterns. Simulations based on the mixed phase model show that the volume fraction of the FE structure should be less than 0.10, even in the case that the FE structure exists in ice VII and the peaks from the FE structure are hidden in the noise level. This constraint is consistent with the estimated volume fraction $f = 0.02$ from high-pressure P-E loop measurement. Although further improvements for background reduction of the neutron diffraction patterns and for more electrical insulation would be necessary to find the potentially existing FE structure, the developed technique opens the way to find interesting properties of ice polymorphs, such as the discovery of a paraferroelectric-type structure transition, which would have a potentially high impact for phase study of not only ice but also many other hydrogen-bonded crystal systems.

We are grateful to all technical staff for their support with the experiments. Neutron diffraction experiments were performed through the ANSTO user programs (Proposals No. 5909 and No. 4684). This research was supported by JSPS KAKENHI (Grants No. 15H05829, No. 16K13904, No. 26246039, No. 18H01936, No. 18H05224, and No. 18J13298).

[1] S. Kawada, J. Phys. Chem. Solids **50**, 1177 (1989).
[2] E. Whalley, J. Chem. Phys. **45**, 3976 (1966).
[3] T. M. Gasser, A. V. Thoeny, L. J. Plaga, K. W. Köster, M. Etter, R. Böhmer, and T. Loerting, Chem Sci. **9**, 4224 (2018).
[4] L. Rosso, M. Celli, and L. Ulivi, Nat. Commun. **7**, 13394 (2016).
[5] A. J. Leadbetter, R. C. Ward, J. W. Clark, P. A. Tucker, T. Matsuo, and H. Suga, J. Chem. Phys. **82**, 424 (1985).
[6] C. G. Salzmann, P. G. Radaelli, E. Mayer, and J. L. Finney, Phys. Rev. Lett. **103**, 105701 (2009).
[7] K. Komatsu, F. Noritake, S. Machida, A. Sano-Furukawa, T. Hattori, R. Yamane, and H. Kagi, Sci. Rep. **6**, 28920 (2016).
[8] C. G. Salzmann, B. Slater, P. G. Radaelli, J. L. Finney, J. J. Shephard, M. Rosillo-Lopez, and J. Hindley, J. Chem. Phys. **145**, 204501 (2016).
[9] P. Pruzan, J. C. Chervin, and M. Gauthier, Europhys. Lett. **13**, 81 (1990).
[10] M. Somayazulu, J. Shu, C. S. Zha, A. F. Goncharov, O. Tschauner, H. K. Mao, and R. J. Hemley, J. Chem. Phys. **128**, 064510 (2008).
[11] H. Fukui, N. Hiraoka, N. Hirao, K. Aoki, and Y. Akahama, Sci. Rep. **6**, 2 (2016).
[12] T. Okada, T. Iitaka, T. Yagi, and K. Aoki, Sci. Rep. **4**, 5778 (2014).
[13] N. Noguchi and T. Okuchi, J. Chem. Phys. **144**, 234503 (2016).
[14] K. Momma and F. Izumi, J. Appl. Crystallogr. **44**, 1272 (2011).
[15] R. Caracas and R. J. Hemley, J. Chem. Phys. **142**, 134501 (2015).
[16] N. Booth, G. Davidson, P. Imperia, S. Lee, B. Stuart, P. Thomas, K. Komatsu, R. Yamane, S. Prescott, H. Maynard-Casely, A. Nelson, and K. Rule, J. Neutron Res. **19**, 49 (2017).
[17] The breakdown at 6–8 kV in runs 3–5 [Fig. 2(b)] might not have occurred in the gaskets but around the PTFE collar and mica sheets, as the corresponding burns were actually observed on the collar and sheets, particularly focused around the corner of anvils. Despite this, we believe that this assembly (using heat-treated pyrophyllite and PTFE gaskets) could be used for higher voltage but optimization of anvil profiles may be necessary to avoid the electric discharge around the corner of the anvils.
[18] S. Klotz, K. Komatsu, H. Kagi, K. Kunc, A. Sano-Furukawa, S. Machida, and T. Hattori, Phys. Rev. B **95**, 174111 (2017).
[19] A. C. Larson and R. B. V. Dreele, GSAS, Technical Report No. LAUR 86-748, Los Alamos National Laboratory, New Mexico, 2004.
[20] B. H. Toby, J. Appl. Crystallogr. **34**, 210 (2001).
[21] R. Yamane, K. Komatsu, and H. Kagi, Rev. Sci. Instrum. **88**, 046104 (2017).
[22] See Supplemental Material at http://link.aps.org/supplemental/10.1103/PhysRevB.99.174201 for a detailed description of the cell assembly for our electric polarization measurements under high pressure.
[23] We conducted P-E loop measurements three times to confirm reproducibility and estimated volume fraction was in the range 0.01–0.02 among the three runs.